Recent Developments of High-Performance NEOMAX Magnets

Y. Kaneko and N. Ishigaki

For further improvement in achieving extremely high magnetic properties of Nd-Fe-B sintered magnets, extensive investigation has been done to densify the magnet up to the theoretical value, to increase the volume fraction of the $Nd_2Fe_{14}B$ matrix phase, and to achieve a high degree of alignment. By controlling chemical composition and the amount of constituent phases, improving particle size distribution, and adopting the isostatic pressing method to get better alignment of fine particles, we have succeeded in obtaining a high-performance magnet having residual flux density (B_r) of 1.495 T (14.95 kG), maximum energy product [$(BH)_{max}$] of 431 kJ/m^3 (54.2 MGOe), and intrinsic coercivity (iH_c) of 845 kA/m (10.62 kOe).

Keywords

densification, high-performance magnets, highest magnetic properties, microstructure, Nd-Fe-B sintered magnets, particles alignment, particle size distribution

1. Introduction

SINCE the invention of Nd-Fe-B sintered magnets (Ref 1) by a conventional powder metallurgical process in 1982, many improvements in composition (Ref 2-4) and protective coating techniques (Ref 5, 6) have been achieved in order to make these magnets more useful for various applications. Nd-Fe-B sintered magnets essentially consist of three basic phases: $Nd_2Fe_{14}B$ phase (T_1), $Nd_{1.1}Fe_4B_4$ phase (T_2), and a neodymium-rich phase (Ref 1). Therefore, the magnetic properties of these magnets depend on the volume fraction of these phases and their orientations.

The theoretical maximum energy product [$(BH)_{max}$] for Nd-Fe-B magnets is calculated to be 512 kJ/m^3 (64 MGOe) based on the saturation magnetization of $Nd_2Fe_{14}B$ single crystal (Ref 7). Several approaches to achieving this value have been tried (Ref 8, 9). In 1987, Sagawa et al. obtained 405 kJ/m^3 (50.6 MGOe) for $Nd_{12.8}Fe_{80.7}B_{6.5}$ [28.74Nd-70.17Fe-1.09B (wt%)] by controlling the oxygen content to less than 1500 ppm. Otsuki et al. achieved 416 kJ/m^3 (52.3 MGOe) in 1990 by a special procedure in which they added neodymium-rich alloy powder, prepared by the rapid-quenching technique, to the alloy powder having a stoichiometric composition of T_1 phase and then sintered the powders. The important points for these works are how to control the composition of magnets to be the stoichiometric T_1 phase and how to achieve a high density. Through a liquid-phase sintering, however, the value of the intrinsic coercivity (iH_c) has been 716 kA/m (9 kOe) at most.

The residual flux density (B_r) of Nd-Fe-B magnets is expressed as (Ref 10, 11):

$$B_r \propto (I_s \cdot \beta) \cdot \{ (\rho/\rho_0) \cdot (1 - \alpha) \}^{2/3} \cdot f \qquad \text{(Eq 1)}$$

where I_s is the saturation magnetization of the T_1 phase, β is the temperature coefficient of the saturated magnetization, ρ is the density of the magnet, ρ_0 is the theoretical value of the density, α is the volume fraction of nonmagnetic phases, $(1 - \alpha)$ is the volume fraction of the T_1 phase, and f is the fraction of T_1 grains aligned in the direction for easy magnetization. In order to enhance B_r in accordance with this equation, it is necessary to densify magnets up to the theoretical value, increase the volume fraction of the T_1 phase, and achieve a high degree of alignment of T_1 grains.

As a result of investigating these items through metallurgical study, we have been able to achieve a high density exceeding 97% and a high volume fraction of T_1 phase up to 95%, while keeping the amount of T_2 and the neodymium-rich phases, which are essential for the liquid-phase sintering, as low as possible. Also, the degree of alignment of T_1 grains has been improved. We have succeeded in developing Nd-Fe-B sintered magnets having the highest magnetic properties of Br = 1.495 T (14.95 kG), $(BH)_{max}$ = 431 kJ/m^3 (54.2 MGOe), and iH_c = 845 kA/m (10.62 kOe).

2. Experimental Procedure

The $(Nd,Pr,Dy)_{12.5\text{-}15}Fe_{77\text{-}81.5}B_{6\text{-}8}$ alloys were prepared by induction melting in an argon atmosphere. The raw materials were 99.5% rare-earth metals, 99.9%-pure electrolytic iron, and ferroboron. As-cast alloys were homogenized in vacuum for 18 ks at 1273 K. The morphology of the alloys was examined by Kerr microscopy, and a part was also measured by differential thermal analysis in an argon atmosphere under heating rates of 0.17 K/s up to 1473 K. The cast alloys were crushed to coarse powder less than 200 μm in diameter by using a jaw crusher and a disk mill, then pulverized by a jet mill to fine powders of about 3 μm in mean particle size. The fine powders were pressed to a cylindrical compact (diameter 5 × 15 mm) in order to measure thermal expansion and contraction. The dimensional changes were measured at the rate of 0.08 K/s up to 1353 K by a dilatometer. Also, the fine powders were pressed to a 10 × 15 × 8 mm rectangular compact in a magnetic field of 800 kA/m, where the pressure was applied perpendicular to the direction of the magnetic field and the direction of the 10 mm length corresponded to the magnetizing direction. The rectan-

Y. Kaneko and **N. Ishigaki**, Research and Development Division, Sumitomo Special Metals Co., Ltd., 2-15-17 Egawa, Shimamoto-cho, Mishima-gun, Osaka, 618 Japan

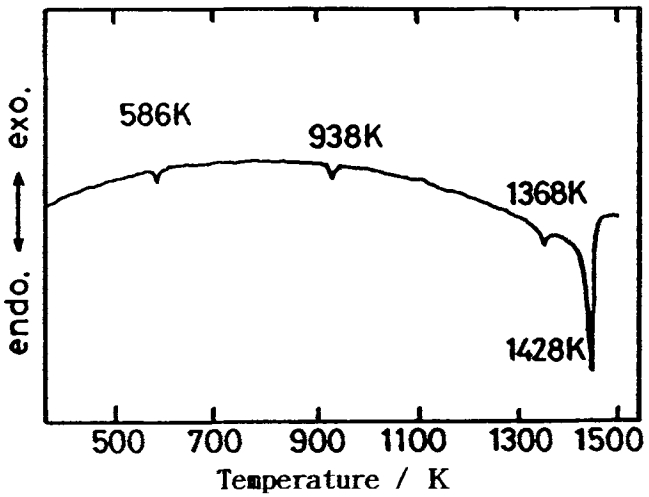

Fig. 1 Differential thermal analysis curve of $Nd_{15}Fe_{78}B_7$ alloy

gular compacts were sintered at about 1333 ~ 1353 K for 10.8 ks in an argon atmosphere and were subsequently annealed at about 773 ~ 873 K for 3.6 ks in argon.

In this study, new techniques for making the fine-powder compacts were carried out. The first technique involved control of the particle size distribution of the fine powders. The second was an isostatic pressing method comprising three steps: (1) powder packing in a cylindrical mold with diameter 25 × 20 mm; (2) alignment with a pulse magnetic field; and (3) isostatic pressing. The compacts obtained by this pressing method were subsequently sintered and annealed. The distribution of the sizes of fine powders was measured by the laser diffraction type particle size analyzer. The magnetic properties were measured by a B-H hysteresis tracer after being fully magnetized by a pulse field of 2.4 MA/m. The microstructure of the heat-treated specimens was investigated by Kerr microscopy and electron probe microanalysis.

3. Results and Discussion

3.1 *Effects of the Constituent Phases of Nd-Fe-B Magnets on the Sintering Behavior and Magnetic Properties*

In order to study the effects of the three basic Nd-Fe-B magnet phases on sintering, a differential thermal analysis was carried out. The result for a $Nd_{15}Fe_{78}B_7$ [32.80Nd-66.05Fe-1.15B (wt%)] alloy is shown in Fig. 1. With increasing temperatures, an endothermic peak appears at 586 K, corresponding to the Curie point of the T_1 phase. Then, a second and third peak appear at 938 and 1368 K, respectively, and finally, a large endothermic reaction occurs at 1428 K. Judging from the previous reports for the Nd-Fe-B ternary diagram (Ref 12, 13), the second peak results from a ternary eutectic reaction of the three constituent phases and the third peak corresponds to a binary eutectic reaction of the T_1 and T_2 phases. The final peak is due to the melting of the T_1 phase.

Figure 2 shows the changes of shrinkage of $Nd_{15}Fe_{78}B_7$ powder compacts from 900 to 1353 K. Shrinkage starts at about

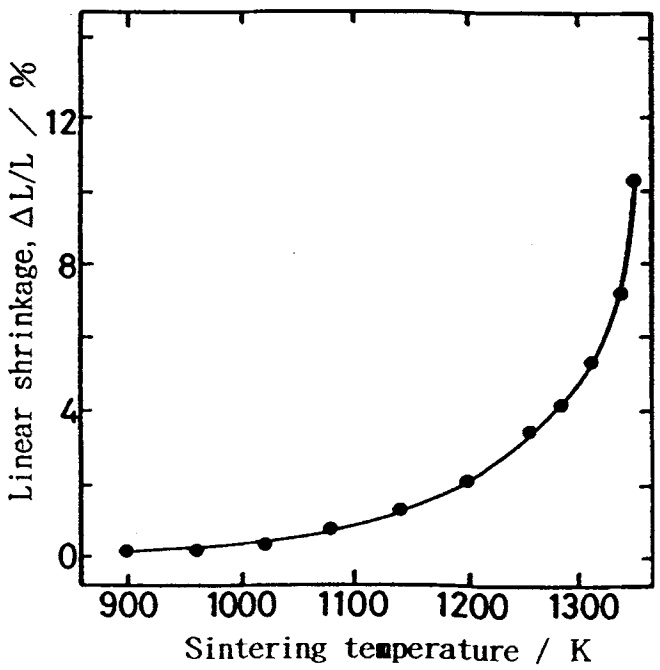

Fig. 2 Linear shrinkage curve of a powder compact of composition $Nd_{15}Fe_{78}B_7$ alloy

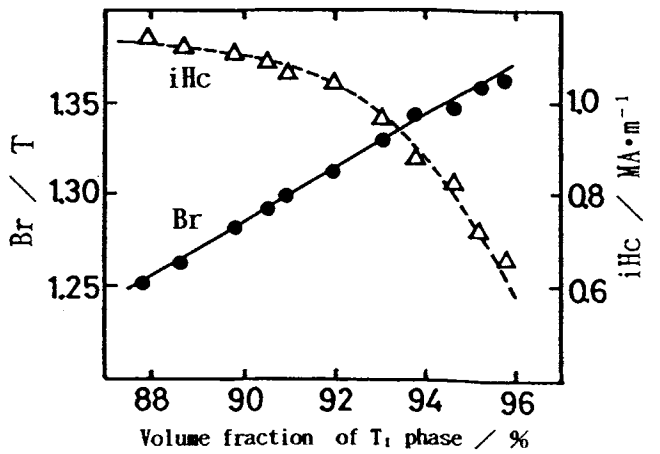

Fig. 3 Dependence of magnetic properties on the volume fraction of the T_1 phase for Nd-Fe-B sintered magnets

950 K and increases gradually with increasing temperatures. Then, a large shrinkage occurs above 1300 K. These experimental results indicate that the sintering of Nd-Fe-B magnets starts at about 940 K due to the formation of a liquid (L) phase by the ternary eutectic reaction of $T_1 + T_2$ + Nd-rich → L. At this stage, however, large densification due to the liquidus flow mechanism cannot occur because of the limited amount of the liquid phase. With increasing sintering temperatures, T_1 grains may react with T_2 grains due to the binary eutectic reaction of $T_1 + T_2 \rightarrow L$. Thus, with increasing amounts of liquid phase, the powder compacts are more rapidly densified through the solution-precipitation mechanism. Consequently, because the three basic constituent phases of T_1, T_2, and neodymium-rich phase

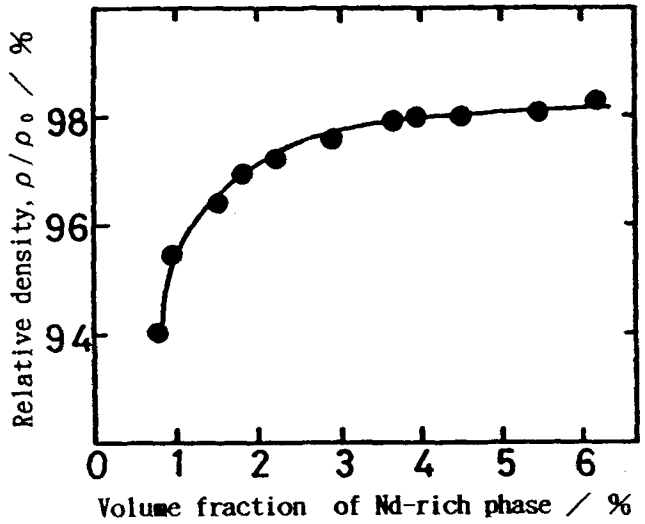

Fig. 4 Relationship between the volume fraction of the neodymium-rich phase and relative density (ρ/ρ_0) for Nd-Fe-B sintered magnets

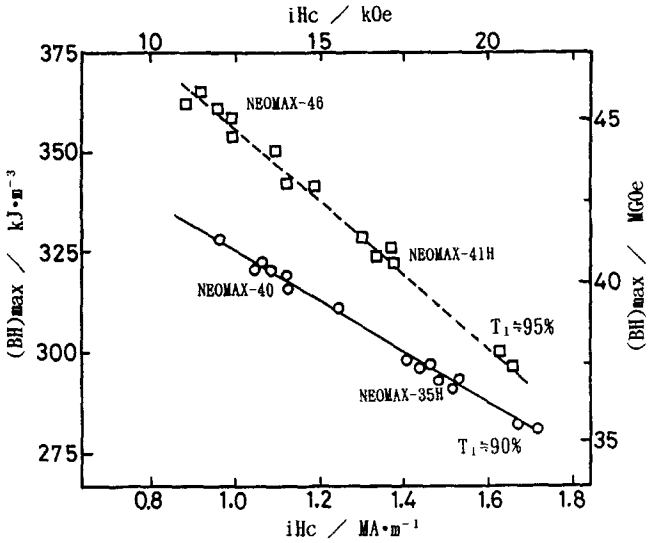

Fig. 5 Intrinsic coercivity (iH_c) and maximum energy product [$(BH)_{max}$)] of Nd-Fe-B sintered magnets as a function of the volume fraction of the T_1 phase. The composition of NEOMAX-46 and -41H is $(Nd,Pr,Dy)_{14.0}Fe_{80.0}B_{6.0}$ and the composition of NEOMAX-40 and -35H is $(Nd, Pr, Dy)_{14.8}Fe_{78.2}B_{7.0}$.

affect the sintering behavior, it is very important to control the amount of these phases in order to obtain a high density, which is the first item needed to obtain high-performance Nd-Fe-B magnets according to Eq 1.

The magnetic properties of Nd-Fe-B magnets are attributable to the T_1 phase and its content in the magnets. Therefore, magnetic measurements were carried out for various compositions of $Nd_xFe_{100-(x+y)}B_y$ where x is about 13 to 15 at.% and y is about 5.9 to 8 at.%. B_r and iH_c are shown in Fig. 3 as a function of the amount of T_1 phase. The amounts of the three constituent phases were estimated from the compositional analysis of T_1

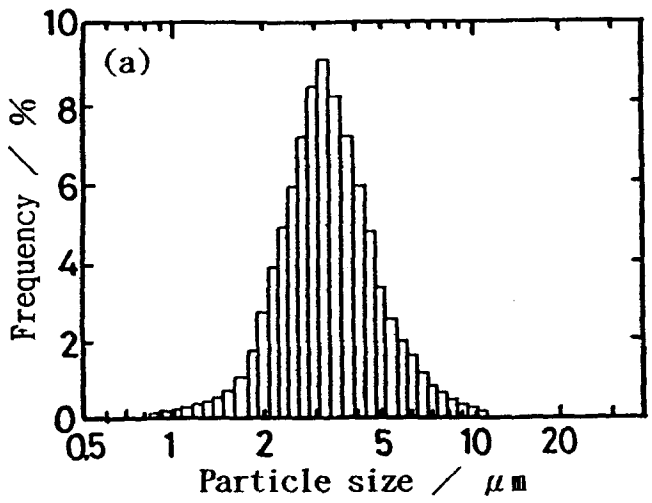

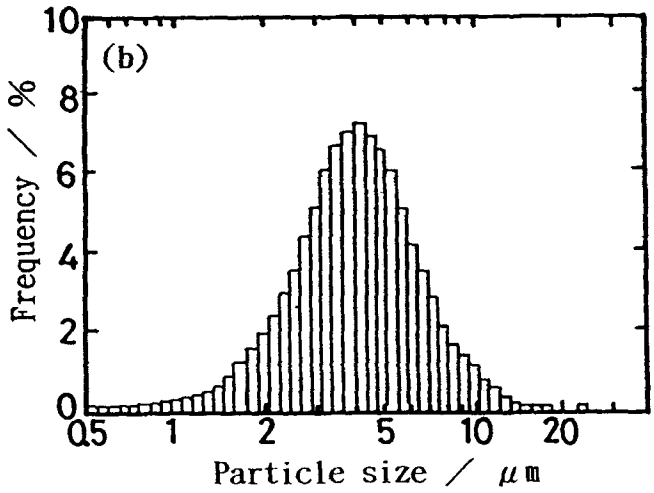

Fig. 6 Particle size distributions of Nd-Fe-B alloy powders prepared by (a) the improved conditions and (b) the conventional conditions

and T_2 phases by assuming that the neodymium-rich phase was neodymium metal (100% Nd). The oxygen involved during the process was also assumed to be used for oxidizing rare-earth elements. It is seen in Fig. 3 that B_r increases linearly with an increasing amount of T_1 phase. This behavior corresponds well to the relation of Eq 1. On the other hand, iH_c decreases gradually with an increasing amount of T_1 phase, up to 93%, but it decreases drastically for the amount beyond 93%. In order to determine the reason for the decrease of iH_c, the relation between the relative density and the amount of neodymium-rich phase is shown in Fig. 4. Here, as the content of oxygen in the specimens was about 4000 ppm, 2.4 wt% of neodymium was consumed by oxidation to form neodymium oxide. It is seen in this figure that the densities of Nd-Fe-B magnets decrease slightly if the amount of neodymium-rich phase is reduced from 6 to 2%. The variation of relative density versus an amount of neodymium-rich phase is similar to that of iH_c versus an amount of neodymium-rich phase. In other words, an increase in the amount of T_1 phase leads to a decrease in the amount of T_2 and neodymium-rich phases to balance. Therefore, the decrease of iH_c is probably due to absence of the liquid phase, leading to a

decrement of T_2 and neodymium-rich phases. In the Nd-Fe-B magnets, whose coercivity is governed by a nucleation-type mechanism, iH_c is influenced significantly by a matching between T_1 matrix phase and grain-boundary phases, and also by the grain size and the morphology of grains (Ref 14, 15).

Consequently, in order to achieve high-performance Nd-Fe-B magnets, it is necessary to increase the amount of T_1 phase up to about 95% while keeping densities and iH_c stable. These are the first and second key technological issues from Eq 1. As shown in Fig. 5, controlling the constituent phases of the Nd-Fe-B magnets and choosing rare-earth elements, such as neodymium, praseodymium, and dysprosium, yields high-performance Nd-Fe-B magnets such as $(BH)_{max} \simeq 366$ kJ/m^3 (46 MGOe), $iH_c > 876$ kA/m (11 kOe) (NEOMAX-46); and $(BH)_{max} \simeq 326$ kJ/m^3 (41 MGOe), $iH_c > 1274$ kA/m (16 kOe) (NEOMAX-41H).

3.2 *Research and Development of Super-High-Energy-Product Magnets*

For further improvement of magnetic properties, the issues are how to increase the value of iH_c without any additives, such as dysprosium, that decrease the saturated magnetization of the $R_2Fe_{14}B$ intermetallic compound (Ref 7), and how to improve the degree of alignment of T_1 grains. We considered that control of the morphology and grain size of the T_1 phase is very effective to increase iH_c, so we studied the crushing and pulverizing conditions for the induction-melting alloys. The particle size distributions obtained by the improved approach and the conventional conditions are shown in Fig. 6. Although the mean particle size of both powders measured by a Fisher subsieve sizer is almost the same, 3 μm, the particle size distribution prepared under the improved conditions is more uniform. As a result, the microstructure of the sintered magnet prepared under the improved pulverizing conditions becomes

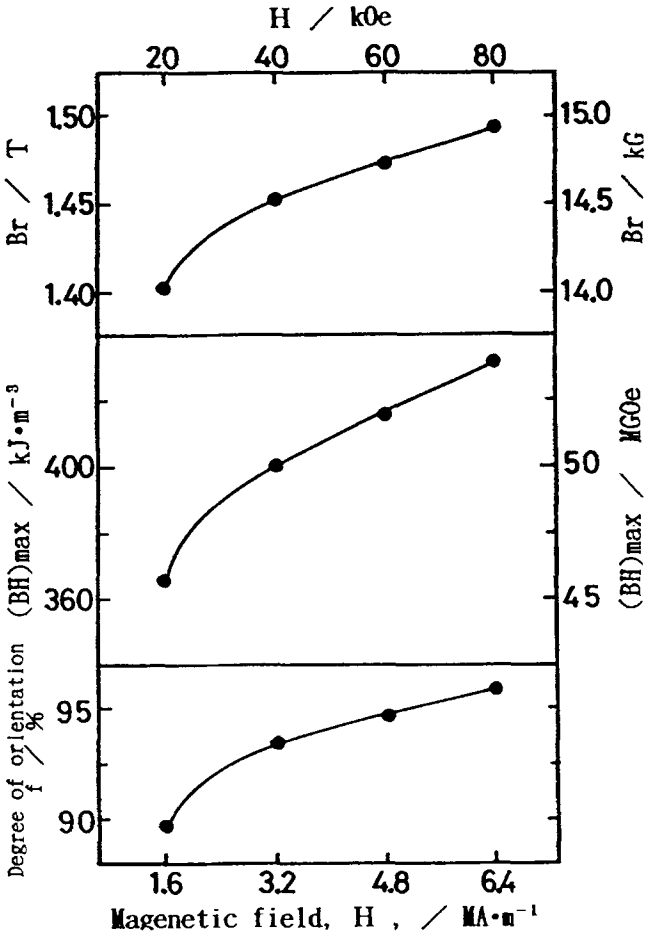

Fig. 7 Relation between the pulse magnetic field and the magnetic properties of an alloy of composition $Nd_{13.1}Fe_{80.9}B_{6.0}$(29.20Nd-69.80Fe-1.00B (wt%) prepared under the improved pulverizing conditions

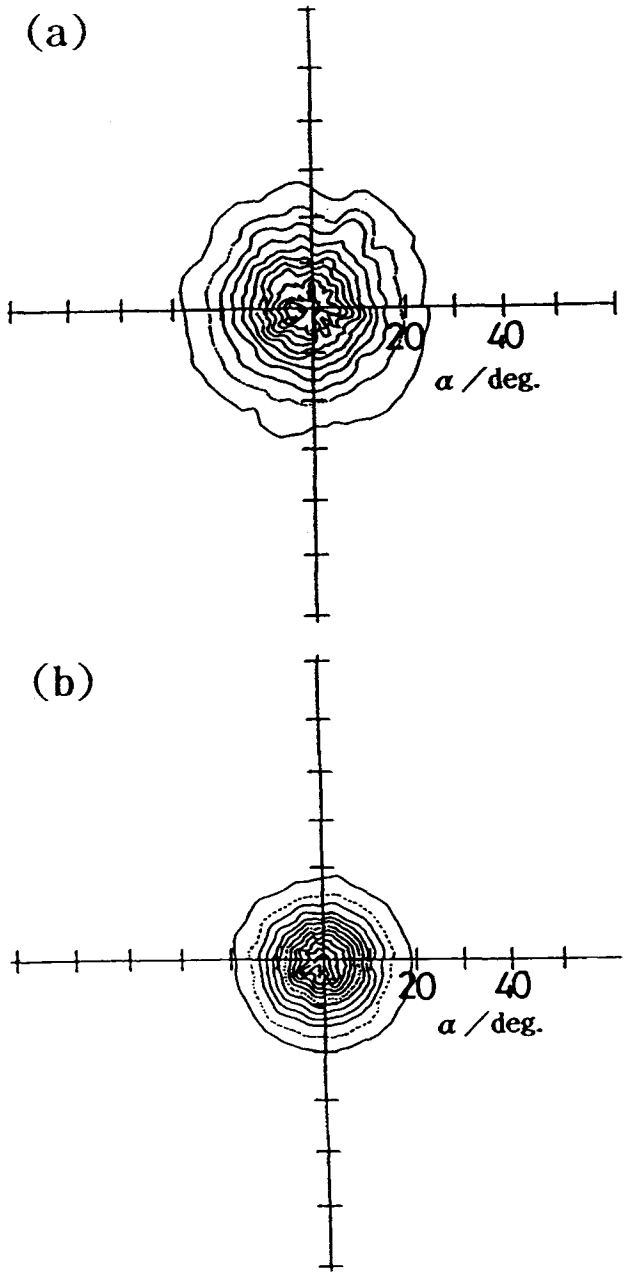

Fig. 8 X-ray pole figures for the (004) diffraction line of a Nd-Fe-B sintered magnet applied with magnetic fields of (a) 1600 kA/m and (b) 6400 kA/m

finer, and the grain size becomes smaller, than under conventional conditions, which results in an increase of iH_c.

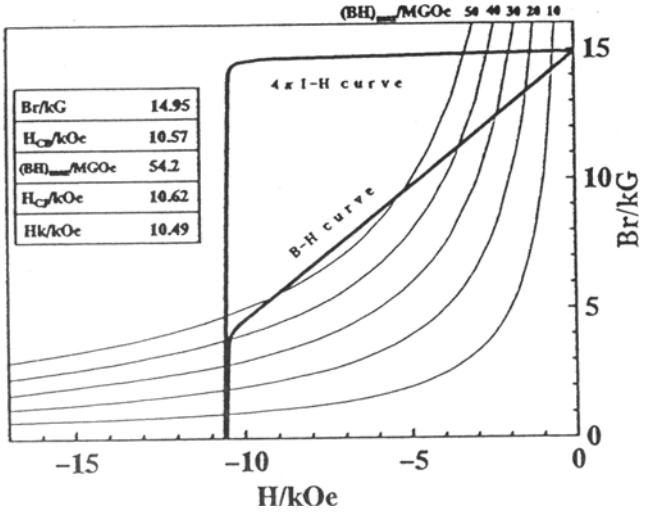

Fig. 9 Demagnetization curve of the newly developed magnet

Also, in order to improve the degree of alignment of T_1 grains up to 95% or more, we investigated the new compacting method for fine powders. Here, the isostatic press was carried out with three steps: (1) filling powders into a cylindrical mold in which the packing density is 2.0 Mg/m^3; (2) aligning with the pulse magnetic field; and finally (3) compacting by isostatic pressing at a pressure of 200 MPa. A pulse magnetic field more than 1600 kA/m was applied in this method. The relation between the pulse magnetic field and the magnetic properties of $Nd_{13.1}Fe_{80.9}B_{6.0}$ prepared under the improved pulverizing conditions is shown in Fig. 7. It is apparent that B_r and $(BH)_{max}$ increase with increasing strength of the pulse field and that the value of $(BH)_{max}$ reaches above 430 kJ/m^3 (54 MGOe). From the results of the calculation of the degree of alignment according to Eq 1, the value of f rises from 90 to 95% with increasing pulse field. On the other hand, the degree of alignment of T_1 grains is evaluated by means of the x-ray pole figure method. In Fig. 8, circular lines correspond to the changes in the intensity of the (004) diffraction line, which is divided into ten levels of relative intensity. In Fig. 8(b), the intensity of (004) at the center of the axis is stronger than in Fig. 8(a), and the distribution of the intensity becomes drastically sharp. In other words, the number of grains deviating from the magnetic alignment direc-

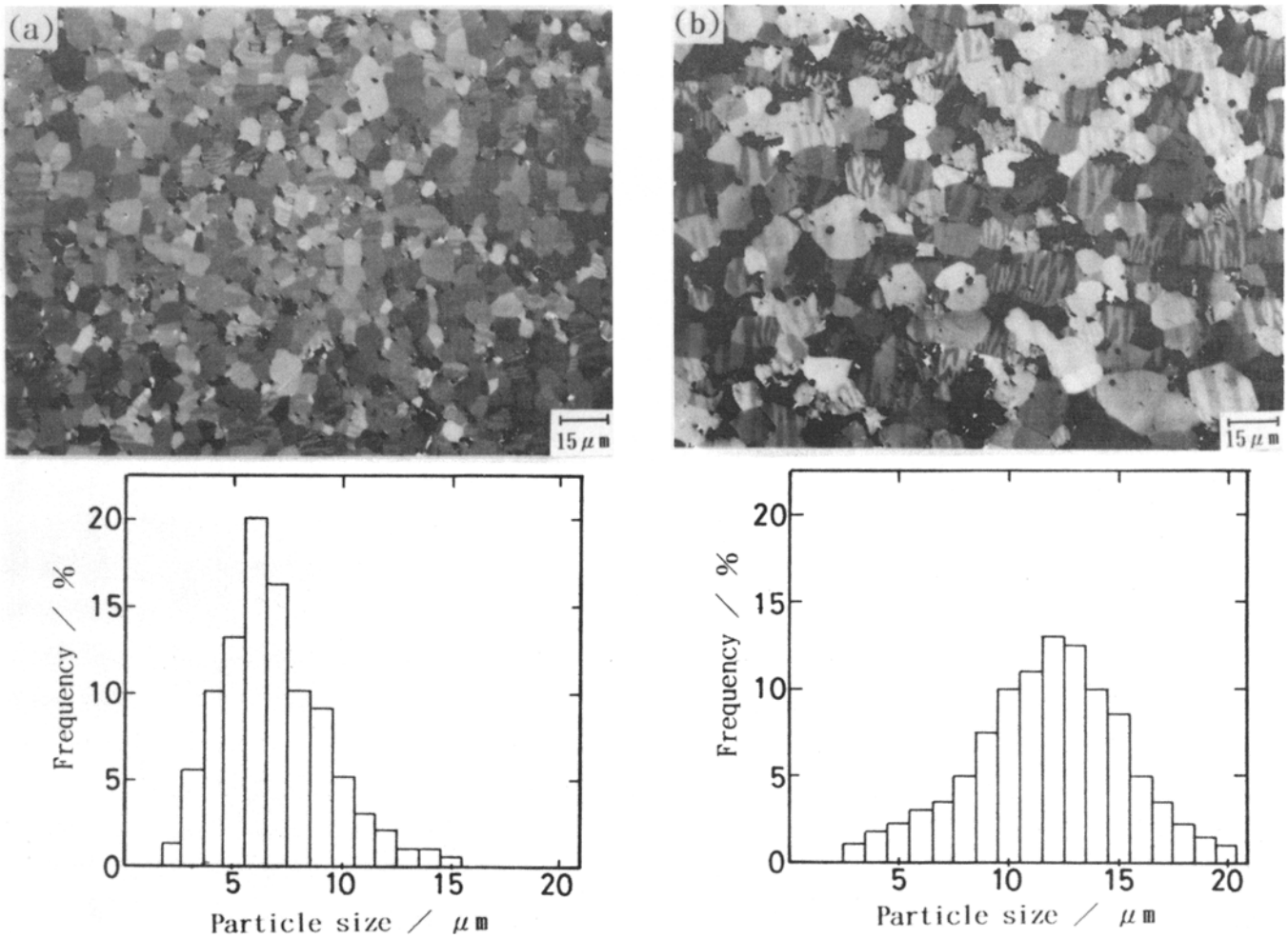

Fig. 10 Microstructure and particle size distributions of (a) the newly developed magnet and (b) the currently mass-produced magnet

tion is lower in the specimen with a magnetic field of 6400 kA/m than in the specimen with a field of 1600 kA/m. Consequently, the improvement of B_r and $(BH)_{max}$ in the specimen prepared by the new process is concluded to be due to the high degree of orientation of T_1 crystals in the Nd-Fe-B magnets.

Based on these additional improvements of the particle size distribution and also the degree of alignment in the Nd-Fe-B magnets, we have achieved the high magnetic properties of B_r = 1.495 T (14.95 kG), $(BH)_{max}$ = 431 kJ/m^3 (54.2 MGOe), and iH_c = 845 kA/m (10.62 kOe), the demagnetization curve of which is shown in Fig. 9. In particular, this magnet has an iH_c exceeding 800 kA/m, which is high compared with previous reports (Ref 8, 9). The newly developed magnet also has a finer microstructure and more uniform particle size distribution than the currently mass-produced magnet (Fig. 10). In conclusion, the key technology in this success is based on the control of the microstructure of the magnets according to Eq 1.

REFERENCES

1. M. Sagawa, S. Fujimura, N. Togawa, H. Yamamoto, and Y. Matsuura, New Material for Permanent Magnets on a Base of Nd and Fe, *J. Appl. Phys.*, Vol 55, 1984, p 2083-2087
2. A. Hasebe and E. Otsuki, Corrosion of Nd-Fe-B Magnets, *Proc. 10th Int. Workshop on Rare Earth Magnets and Their Applications* (Kyoto), Vol 2, 1989, p 383
3. S. Hirosawa, S. Mino, and H. Tomizawa, Improved Corrosion Resistance and Magnetic Properties of Nd-Fe-B-type Sintered Magnets with Mo and Co, *J. Appl. Phys.*, Vol 69, 1991, p 5844-5846
4. P. Tenaudo, F. Vial, and M. Sagawa, Improved Corrosion and Temperature Behaviour of Modified Nd-Fe-B Magnets, *IEEE Trans. Magn.*, Vol MAG-26, 1990, p 1930-1932
5. W. Bloch, K. Grendel, and H. Staubach, Corrosion Protection of Nd-Fe-B Magnets by Coating, *Proc. 11th Int. Workshop on Rare Earth Magnets and Their Applications* (Pittsburgh), Vol 1, 1990, p 108-122
6. K. Tokuhara and S. Hirosawa, Corrosion Resistance of Nd-Fe-B Sintered Magnets, *J. Appl. Phys.*, Vol 69 (No. 8), 1991, p 5521-5523
7. M. Sagawa, S. Fujimura, H. Yamamoto, Y. Matsuura, and S. Hirosawa, Magnetic Properties of Rare-Earth-Iron-Boron Permanent Magnets, *J. Appl. Phys.*, Vol 57, 1985, p 4094-4096
8. M. Sagawa, S. Hirosawa, H. Yamamoto, S. Fujimura, and Y. Matsuura, Nd-Fe-B Permanent Magnet Materials, *Jpn. J. Appl. Phys.*, Vol 26, 1987, p 785-800
9. E. Otsuki, T. Otsuka, and T. Imai, Processing and Magnetic Properties of Sintered Nd-Fe-B Magnets, *Proc. 11th. Int. Workshop on Rare Earth Magnets and Their Applications* (Pittsburgh), Vol 1, 1990, p 328-340
10. H. Taguchi, "Nihon Denshi Zairyo Kogyokai," unpublished research report, 1990, p 38-39 (in Japanese)
11. Y. Kaneko, K. Kitajima, and N. Takusagawa, Preparation of Sr-Ferrite Magnets by the New Annealing-Remilling Process, *J. Ceram. Soc. Jpn.*, Vol 101, 1993, p 905-912 (in Japanese)
12. Y. Matsuura, S. Hirosawa, H. Yamamoto, S. Fujimura, M. Sagawa, and K. Osamura, Phase Diagram of the Nd-Fe-B Ternary System, *Jpn. J. Appl. Phys.*, Vol 24, 1985, p L635-639
13. H. Stadelmier, N. Elmasley, N. Lle, and S. Cheng, The Metallurgy of the Iron-Neodymium-Boron Permanent Magnet System, *Mater. Lett.*, Vol 2, 1984, p 411
14. S. Hirosawa and Y. Tsubokawa, The Nd-Fe-B Materials for Permanent Magnets, *J. Magn. Magn. Mat.*, Vol 84, 1990, p 4094
15. S. Hirosawa, On the Dependence of Intrinsic Coercivity on Grain Size in the Nucleation-Controlled Rare Earth-Iron-Born Sintered Magnets, *IEEE Trans. Magn.*, Vol MAG-25, 1989, p 3437